Development of New Photocatalytic Water Splitting into H_2 and O_2 using Two Different Semiconductor Photocatalysts and a Shuttle Redox Mediator IO_3^-/I^-

Ryu Abe,* Kazuhiro Sayama, and Hideki Sugihara

National Institute of Advanced Industrial Science and Technology (AIST), 1-1-1 Higashi, Tsukuba, Ibaraki 305-8565, Japan

Received: May 30, 2005

A new type of photocatalytic reaction that splits water into H_2 and O_2 was designed using a two-step photoexcitation system composed of an iodate/iodide (IO_3^-/I^-) shuttle redox mediator and two different photocatalysts, one for H_2 evolution and the other for O_2 evolution. Photocatalytic oxidation of water to O_2 and reduction of IO_3^- to I^- selectively proceeded with good efficiencies over TiO_2-rutile and Pt-WO_3 photocatalysts under UV and visible light irradiations, respectively. The O_2 evolution selectively proceeded even in the presence of a considerable amount of I^- in the solutions, although the oxidation of water is thermodynamically less favorable than oxidation of I^-. Both the adsorption property of IO_3^- anions and the oxidation property of the photocatalysts are doubtless responsible for the selective oxidation of water. On the other hand, photocatalytic reduction of water to H_2 and oxidation of I^- to IO_3^- proceeded over Pt-TiO_2-anatase and Pt-$SrTiO_3$:Cr/Ta (codoped with Cr and Ta) photocatalysts under UV and visible light, respectively. The combination of two different photocatalysts results in a stoichiometric evolution of H_2 and O_2 via the redox cycle of IO_3^- and I^-. The photocatalytic water splitting under visible light irradiation ($\lambda > 420$ nm) was demonstrated by using the Pt-$SrTiO_3$:Cr/Ta, Pt-WO_3, and IO_3^-/I^- shuttle redox mediator.

Introduction

Photocatalytic splitting of water into H_2 and O_2 by semiconductors has received much attention because of the potential production of clean fuel H_2 from water utilizing solar energy.[1−10] The development of a photocatalyst system that can efficiently function in visible light ($\lambda > 400$ nm), which occupies almost half the solar spectrum, is indispensable for practical utilization of solar light.

A two-step water splitting system utilizing a reversible redox couple (A/D) shown in Figure 1a, mimicking a system of the Z-scheme mechanism of photosynthesis, is possibly the most promising way of achieving photocatalytic water splitting under visible light due to the reduction of energy required for both processes.[11−20] Over the H_2 evolution photocatalyst, water is reduced to H_2 by photoexcited electrons, and the electron donor (D) is then oxidized to an electron acceptor (A) by holes. On the O_2 evolution photocatalyst, the photoexcited electrons reduce the electron acceptor (A) back to the electron donor (D), while holes oxidize water to O_2. However, the demonstration of the simultaneous evolution of H_2 and O_2 is extremely difficult in the two-step water splitting system because backward reactions easily proceed over each photocatalyst, as shown in Figure 2.[12−14,16,17] Over the H_2 evolution photocatalyst, the desirable forward reactions, the reduction of H^+ to H_2, and the oxidation of D to A (shown in Figure 2 as a solid line), proceed only in an initial period where the solution contains mainly D. The H_2 evolution terminates when the concentration of A in the solution reaches a certain level. The reduction of the A to D (shown in Figure 2 as broken lines), a thermodynamically advantageous backward reaction, proceeds preferentially instead of the reduction of H^+. On the contrary, the rate of O_2 evolution over the O_2 evolution photocatalyst decreases with the increasing concentration of D in the solution because of the backward oxidation of D to A. To realize the two-step water splitting system, it is therefore necessary to construct the photocatalytic system with a high selectivity for the forward reactions. With this strategy, we had first demonstrated the two-step water splitting into H_2 and O_2 by combining two different photocatalysts and an iodate/iodide (IO_3^-/I^-) shuttle redox mediator,[18,19] and Kudo et al. have recently reported the two-step water splitting using iron redox mediator (Fe^{3+}/Fe^{2+}).[20]

In the present study, the detailed mechanism of the two-step water splitting into H_2 and O_2 using two different photocatalysts and an iodate/iodide (IO_3^-/I^-) shuttle redox mediator is investigated. First, we report the selective and efficient O_2 evolution over TiO_2-rutile and Pt-WO_3 photocatalysts using IO_3^- as an electron acceptor, the key process of achieving a two-step water splitting system using a shuttle redox mediator. The reaction selectivity is discussed from the standpoints of the adsorption properties of the IO_3^-/I^- redox and the oxidation properties of photocatalysts. We finally combine two visible-light driven photocatalysts, Pt-$SrTiO_3$:Cr/Ta for H_2 evolution and Pt-WO_3 for O_2 evolution, using the IO_3^-/I^- shuttle redox mediator and demonstrate the photocatalytic water splitting into H_2 and O_2 under visible light irradiation.

Experimental Procedures

Materials. Commercially available TiO_2 powders such as TiO_2-A1 (anatase, 320 m^2/g, Ishihara Co. Ltd. ST-01), TiO_2-R1 (rutile, 40 m^2/g, Ishihara Co. Ltd. TTO-55N), and TiO_2-R2 (rutile, 2 m^2/g, Toho titanium Co. Ltd. HT0210) were used.

* Corresponding author. Phone: 81-298-61-9405; fax: 81-298-61-4750; e-mail: r-abe@aist.go.jp.

10.1021/jp052848l CCC: $30.25
Published on Web 08/02/2005

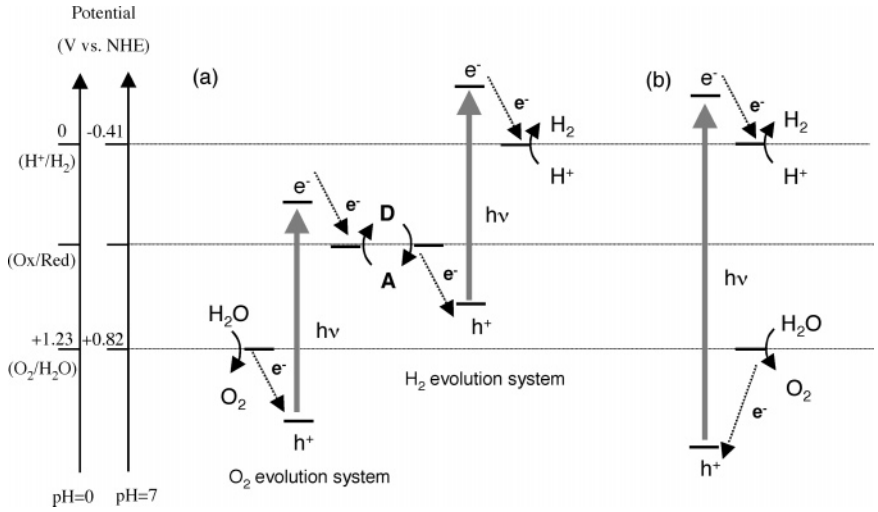

Figure 1. Conceptual scheme of water splitting systems: (a) two-step system and (b) one-step system.

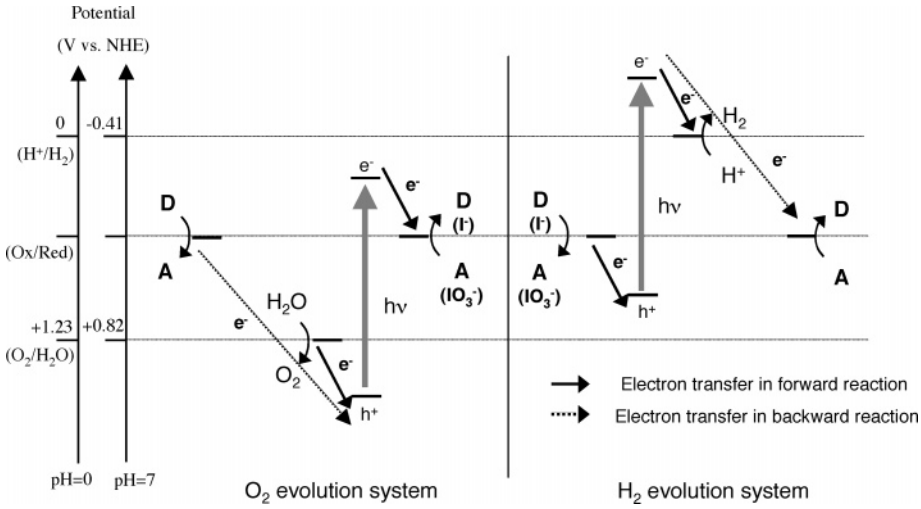

Figure 2. Forward and backward reactions that take place over semiconductor photocatalysts in the two-step water-splitting system.

The TiO_2-anatase photocatalyst (48 m^2/g), hereafter denoted TiO_2-A2, was prepared by hydrolysis of titanium tetra-propoxide in a distilled water solution followed by air-drying and calcination at 500 °C for 1 h. A WO_3 powder (99.99%) was provided by Koujyundo Chemical. Other chemicals used in these experiments were purchased from commercial sources as guaranteed reagents and used without any further purification. Monoclinic $BiVO_4$ and a $SrTiO_3$ codoped with chromium/tantalum (denoted hereafter as $SrTiO_3$:Cr/Ta) were prepared according to the reports by Kudo et al.[21−23] Pt-loaded TiO_2 and $SrTiO_3$:Cr/Ta photocatalysts were prepared by a photochemical deposition method. The powder photocatalyst was stirred in a 1% methanol aqueous solution containing H_2PtCl_6 and irradiated by a high-pressure Hg lamp for 12 h. Photoreduction of H_2PtCl_6 took place, and highly dispersed Pt metal particles were deposited on the surface of the photocatalyst. After filtrating and washing by distilled water, the powder was evacuated at 200 °C for 2 h to remove the methanol adsorbed on the surface of the catalyst. The preparation of Pt-loaded WO_3 and $BiVO_4$ was carried out by an impregnation method from H_2PtCl_6 aqueous solutions followed by calcination in air at 500 °C for 1 h.

Photocatalytic Reaction. The photocatalytic reactions were performed using a closed gas-circulating system with two different types of reactors. The photocatalytic reaction under UV irradiation was carried out using an inner irradiation type reactor, in which a light source (400 W high-pressure Hg lamp, Riko Kagaku) was covered with a Pyrex glass-made cooling water jacket (cutoff $\lambda < 300$ nm) to keep the reactor temperature constant at 20 °C. The reaction under visible light irradiation was performed using a Pyrex glass-made outer irradiation type reactor. The irradiation to the aqueous suspension of catalyst was carried out from outside the reactor using a 300 W xenon lamp through a water filter and a UV cutoff filter. The photocatalyst powder was suspended in distilled water using a magnetic stirrer, and the required amount of solute, such as NaI, was added to the suspension. The pH of the solution was adjusted to a fixed value between 3 and 13 using H_2SO_4 or NaOH. Finally, the suspension was thoroughly degassed after which argon gas (35 Torr) was introduced into the system and exposed to irradiation. Evolved H_2 and O_2 gases were analyzed by on-line gas chromatography (TCD, molecular sieve 5A, Ar carrier). The amount of I_3^- and IO_3^- anions produced after reactions were determined by UV−vis absorption spectroscopy and ion chromatography (Shimadzu SPD-6AV, UV at 240 nm, column IC-A1) using a Na_2HPO_4 aqueous solution as the mobile phase.

The quantum yield was determined using a Pyrex outer irradiation type reactor under the irradiation of monochromatic light obtained through two band-pass filters. The light intensity was measured with a thermopile power meter.

Photoelectrochemical Measurements. To study photoelectrochemical properties of TiO_2 photocatalysts, porous TiO_2 film

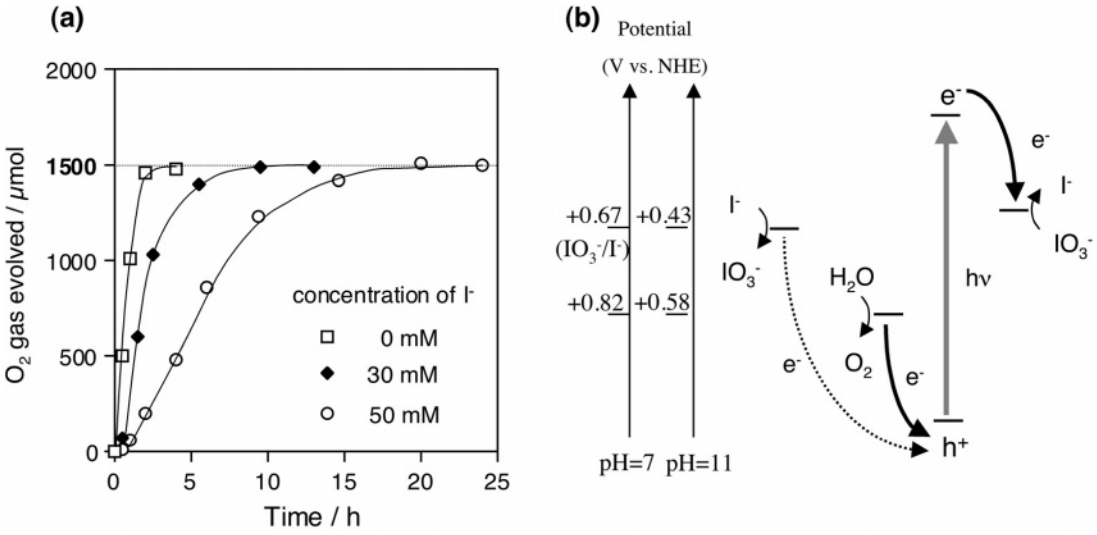

Figure 3. (a) Photocatalytic O_2 evolution over TiO_2-R2 photocatalyst using iodate (IO_3^-) as the electron acceptor under UV light irradiation. The reaction was carried out in aqueous solution (400 mL, pH = 11 adjusted by NaOH) containing $NaIO_3$ (2.5 mM) and NaI (0, 30, and 50 mM). The broken line shows the upper limit of O_2 evolution expected from the amount of IO_3^- added to the solutions. (b) Energy diagram of O_2 evolution over a semiconductor photocatalyst in the presence of IO_3^- and I^- anions.

electrodes were prepared by spreading a viscous slurry of TiO_2 paste on conducting glass supports (F-doped SnO_2). They were then dried and calcined at 500 °C for 1 h. A platinum wire and an Ag/AgCl electrode were used as a counter and a reference electrode, respectively. The Pt counter electrode was separated from the TiO_2 electrode by an ion-exchange membrane (Nafion). The potential of the TiO_2 electrodes was controlled by a potentiostat. The Na_2SO_4 aqueous solution (10 mM, pH 11 adjusted by NaOH) was used as an electrolyte solution for electrochemical measurements. The solution was purged with nitrogen gas for more than 30 min before the measurements.

Results and Discussion

Selective Water Oxidation Over TiO_2-Rutile and WO_3 Photocatalysts in an Aqueous Solution Containing Both IO_3^- and I^- Anions. We investigated photocatalytic H_2 or O_2 evolutions using various semiconductor photocatalysts suspended in an aqueous solution containing an electron donor (D) or an electron acceptor (A). In most cases, the gas evolution readily terminated when the concentration of the product in the solution reached a certain level because of the backward reactions, shown in Figure 2. However, we found that efficient and selective O_2 evolution proceeded over TiO_2-rutile photocatalysts in the aqueous solution (pH 7 to ~13) containing an IO_3^- anion as an electron acceptor (A) with the following reactions:

$$h\nu \rightarrow e^- + h^+ \text{ (photoexcitation of photocatalyst)} \quad (1)$$

$$IO_3^- + 3H_2O + 6e^- \rightarrow I^- + 6OH^- \text{ (reduction of } IO_3^- \text{ to } I^- \text{ by electrons)} \quad (2)$$

$$2H_2O + 4h^+ \rightarrow O_2 + 4H^+ \text{ (oxidation of water to } O_2 \text{ by holes)} \quad (3)$$

Figure 3a shows time courses of O_2 evolution over the TiO_2-R2 photocatalyst in the aqueous solution (400 mL, pH 11) containing 1 mmol of $NaIO_3$ under UV light irradiation. When the reaction was initiated in the absence of I^- anions, O_2 evolution proceeded with a fairly high efficiency (rate of O_2 evolution: ca. 1 mmol/h, Q.E. at 350 nm: ca. 10%). The O_2 evolution continued until the total amount of O_2 gas reached 1.5 mmol, agreeing with the stoichiometric amount expected from the amount of IO_3^- anions (1 mmol) in the solution. No IO_3^- anion was detected in the solution after the photoreaction. These results indicate that the photocatalytic oxidation of water over TiO_2-R2 proceeded until almost all IO_3^- anions in the solution were reduced into I^- anions. Interestingly, the O_2 evolution over TiO_2-R2 continued until the total amount of O_2 gas reached 1.5 mmol even when considerable amounts of I^- anions were present in the solution, as shown in Figure 3a, while the rate of O_2 evolution was lowered to some extent by the increase in the I^- concentration. This behavior of the TiO_2-rutile photocatalyst is very unique from the thermodynamic standpoint of the reactions, as shown in Figure 3b. The oxidation of water, which is a thermodynamically less favorable reaction as compared with the oxidation of I^-, preferentially proceeded over TiO_2-R2 even in the presence of I^-. On the other hand, the preferential oxidation of water was not observed over TiO_2-anatase photocatalysts. Figure 4 shows the rates of O_2 evolution over TiO_2 photocatalysts in the solution containing both IO_3^- and I^- anions. The rates of O_2 evolution over TiO_2-anatase photocatalysts markedly decreased with the increasing concentration of I^-. The O_2 evolution was negligible when the concentration of I^- was above 40 mM, in the case of TiO_2-A1, or 10 mM, in the case of TiO_2-A2, while steady O_2 evolution was observed over TiO_2-rutile photocatalysts even with the I^- concentration above 50 mM. It is thus presumed that over TiO_2-anatase photocatalysts, the oxidation of I^-, which is a thermodynamically favorable reaction, proceeds preferentially in the aqueous solution containing a considerable amount of I^-.

$$I^- + 6OH^- + 6h^+ \rightarrow IO_3^- + 3H_2O \text{ (backward oxidation of } I^- \text{ to } IO_3^-) \quad (4)$$

Consequently, the undesirable recycled reaction ($IO_3^- \leftrightarrow I^-$, a combination of reactions 2 and 4), which consumes electrons (e^-) and holes (h^+), occurred over TiO_2-anatase photocatalysts instead of O_2 evolution. It should be noted that TiO_2-A2 (surface area: 48 m^2/g) and TiO_2-R1 (surface area: 40 m^2/g), which have similar surface areas, show quite different reactivity.

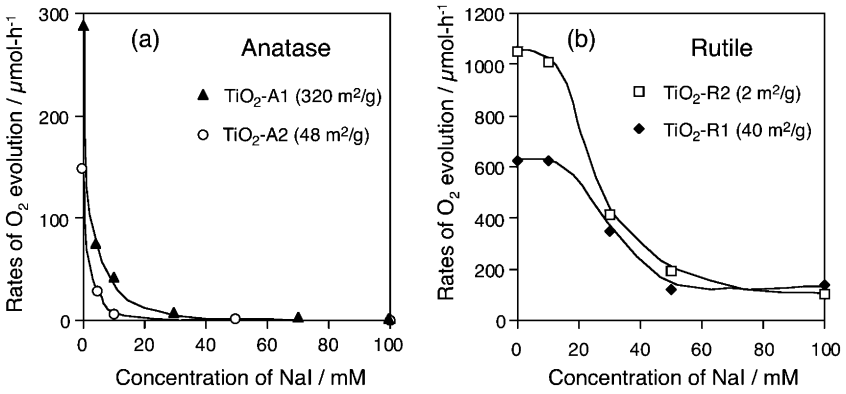

Figure 4. Rates of O_2 evolution over TiO_2 photocatalysts in the solutions (pH = 11) containing both 2.5 mM $NaIO_3$ and different concentrations of NaI between 0 and 100 mM under UV light irradiation (λ > 300 nm, 400 W Hg lamp).

TABLE 1: Rates of O_2 Evolution over WO_3 and $BiVO_4$ Photocatalysts Suspended in $NaIO_3$ (4 mM) Aqueous Solution under Visible Light Irradiation[a]

catalyst	rates of O_2 evolution (μmol)
WO_3	tr.[b]
Pt(0.5 wt %)-WO_3	75
RuO_2(0.5 wt %)-WO_3	22
IrO_2(0.5 wt %)-WO_3	15
$BiVO_4$	2.1
Pt(0.5 wt %)-$BiVO_4$	22
RuO_2(0.5 wt %)-$BiVO_4$	10
IrO_2-(0.5 wt %)-$BiVO_4$	20
WO_3 (Ag^+ acceptor)	126[c]
$BiVO_4$ (Ag^+ acceptor)	240

[a] Catalyst: 0.25 g of water: 250 mL. [b] $NaIO_3$: 1 mmol. [c] $AgNO_3$: 2.5 mmol of Pyrex reactor of outer irradiation type. Xe lamp (300 W) with cut-off filter (>420 nm).

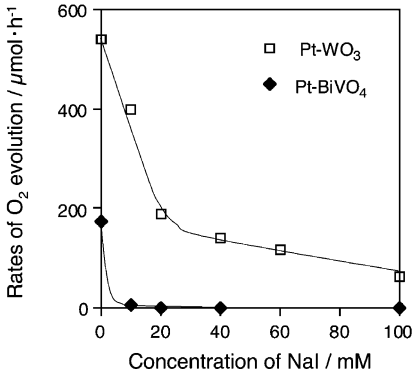

Figure 5. Rates of O_2 evolution over Pt(0.5 wt %)-WO_3 and Pt(0.5 wt %)-$BiVO_4$ photocatalysts in the solutions (without pH adjustment) containing both 2.5 mM $NaIO_3$ and different concentrations of NaI between 0 and 100 mM under UV light irradiation.

Therefore, the factor governing the reactivity undoubtedly rests on the difference in the crystal form instead of the surface area.

We found that the selective oxidation of water also proceeds over the WO_3 photocatalyst. As shown in Table 1, the WO_3 and $BiVO_4$ photocatalysts showed activity for water oxidation to O_2 in the presence of IO_3^- as an electron acceptor under visible light irradiation (λ > 420 nm), although the loading of a cocatalyst, such as Pt, was indispensable for efficient O_2 evolution. When the reaction was carried out in the presence of I^- anions, the Pt-WO_3 and Pt-$BiVO_4$ photocatalysts showed quite different reactivity to each other. The reaction was carried out in aqueous solution with a neutral pH around 7 because WO_3 is unstable in alkaline conditions. As shown in Figure 5, the O_2 evolution over Pt-$BiVO_4$ under UV light irradiation was significantly suppressed by the addition of I^- anions into the initial $NaIO_3$ aqueous solution, similar to the case of TiO_2-anatase photocatalysts. This suggests that the backward reaction, oxidation of I^- to IO_3^- (or I_3^-), preferentially proceeds over the Pt-$BiVO_4$ photocatalyst instead of the oxidation of water. On the other hand, Pt-WO_3 can produce O_2 even in the presence of a considerable amount of I^- in the solution, as in the case of TiO_2-rutile photocatalysts. A similar trend was observed under visible light irradiation.

We also investigated photocatalytic O_2 evolution using I_3^- as an electron donor instead of the IO_3^- anion.

$$I_3^- + 2e^- \rightarrow 3I^- \text{ (reduction of } I_3^- \text{ to } I^- \text{ by electrons)} \quad (5)$$

However, efficient O_2 evolution was not observed over any photocatalysts examined, despite the similar standard potential of the I_3^-/I^- redox couple (+0.54 V vs NHE at pH 7) to that of IO_3^-/I^- (+0.67 V vs NHE at pH 7).

From these results, we can conclude that the TiO_2-rutile and Pt-WO_3 photocatalysts have a unique property of oxidation, which enables preferential oxidation of water to produce O_2 in the presence of both IO_3^- and I^-, regardless of the thermodynamic disadvantage of water oxidation when compared to the oxidation of I^-. This is a desired property in a photocatalyst for an O_2 evolution system and is useful to achieve two-step water splitting as shown in Figure 1.

Unique Adsorption Property of IO_3^- Anion onto Photocatalysts. To clarify the reason for efficient and selective water oxidation over the TiO_2-rutile photocatalysts in the presence of both IO_3^- and I^-, we measured the adsorptivity of IO_3^- and I^- anions on TiO_2-R2. The amounts of IO_3^- and I^- anions adsorbed on TiO_2-R2 were determined by analyzing the concentration of the anions in the solutions before and after the addition of measured amounts of TiO_2 powder to the solutions while in darkness. As shown in Figure 6a, the IO_3^- anions are easily adsorbed on the surface of TiO_2-R2, while I^- anions show a much lower adsorptivity. The adsorption isotherm of the IO_3^- anions indicates that the adsorption of IO_3^- onto TiO_2-R2 almost saturates with the concentration above 0.3 mM. Figure 6b shows the initial rates of O_2 evolution over the TiO_2-R2 photocatalyst in the presence of various concentrations of IO_3^- anions. The rate of O_2 evolution is almost independent of the concentration of IO_3^- anions. An efficient O_2 evolution proceeds even in the solution containing only 0.1 mM IO_3^-.

The preferential adsorption of IO_3^- was also observed on the Pt-WO_3 photocatalyst. The initial rate of O_2 evolution under visible light irradiation (λ > 420 nm) was almost independent of the IO_3^- concentration as shown in Figure 7. It should be

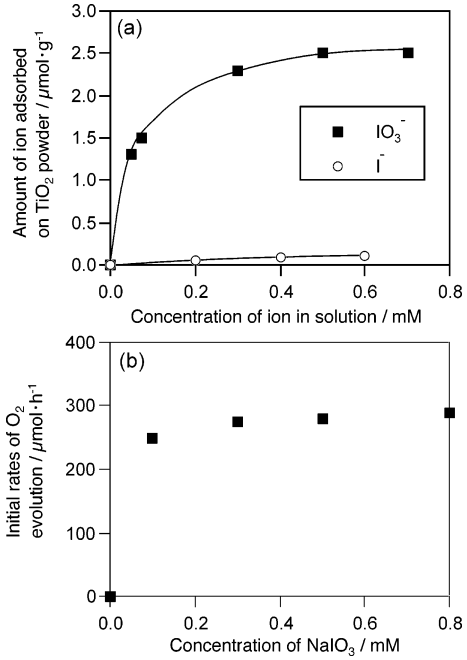

Figure 6. (a) Adsorption isotherms of IO_3^- and I^- anions on TiO_2-R2 powder at 25 °C. (b) Initial rates of O_2 evolution over TiO_2-R2 in the solutions (pH = 11) containing both 50 mM NaI and different concentrations of $NaIO_3$ under UV light irradiation.

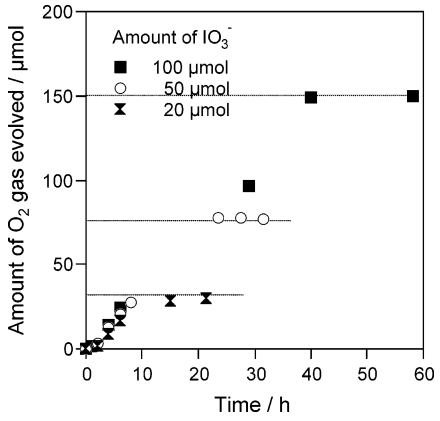

Figure 7. Photocatalytic O_2 evolution over Pt(0.5 wt %)-WO_3 using iodate (IO_3^-) as the electron acceptor at different concentrations under visible light irradiation (λ > 420 nm). The reaction was carried out in aqueous solution (250 mL) containing NaI (10 mM) and $NaIO_3$ (0.4, 0.2, and 0.08 mM). The broken lines show the upper limits of O_2 evolution expected from the amount of IO_3^- added to the solutions.

noted that the O_2 evolution over the Pt-WO_3 photocatalyst continued until almost all IO_3^- anions in the solution were reduced to I^-, as in the case of TiO_2-rutile. For example, the amount of O_2 reached the expected value (35 μmol) even when the reaction was carried out in the presence of quite small amounts of IO_3^- (20 μmol).

We can therefore conclude that the IO_3^- anions in the solution, even in low concentrations, easily adsorbed onto the surface of TiO_2-rutile and Pt-WO_3 photocatalysts and efficiently reacted with the photogenerated electrons there. Consequently, efficient O_2 evolution proceeded over the TiO_2-rutile and Pt-WO_3 photocatalysts. On the other hand, we could not observe such a preferential adsorption property of I_3^- anions onto the photocatalysts. The poor adsorption property of I_3^- anions is certainly due to the quite low efficiency of O_2 evolution over the photocatalysts using I_3^- anions as the electron acceptors. The adsorption property of IO_3^- anions is most certainly one

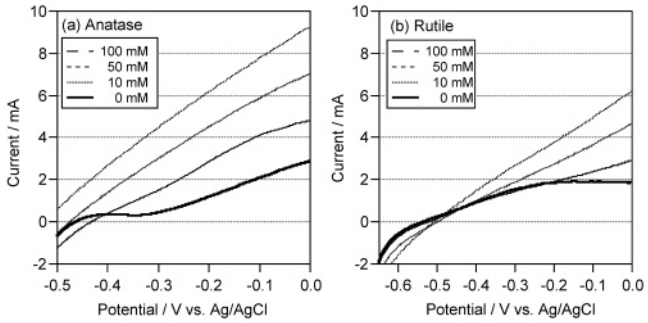

Figure 8. I−V characteristics of porous TiO_2 electrodes (ca. 4 cm^2) in an aqueous solution containing different concentrations of NaI from 0 to 100 mM (pH = 11 adjusted by NaOH).

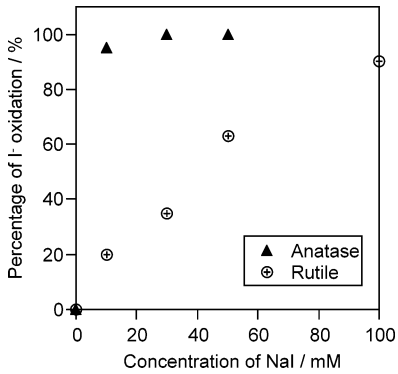

Figure 9. Percentage of oxidation of I^- to the total oxidation current on TiO_2 electrodes in a solution containing different concentrations of NaI (pH = 11, adjusted with NaOH).

of the reasons for efficient and selective water oxidation over the TiO_2-rutile and Pt-WO_3 photocatalysts in the presence of both IO_3^- and I^-. However, the preferential adsorption of IO_3^- was observed not only on TiO_2-rutile but also on TiO_2-anatase. Therefore, another factor will contribute to the efficient and selective O_2 evolution over TiO_2-rutile.

Different Reactivity in Oxidation between TiO_2-Anatase and Rutile. To clarify the different reactivity in oxidation over anatase and rutile, photoelectrochemical measurements were conducted using two porous TiO_2 photoelectrodes made of TiO_2-A2 and TiO_2-R1 powders with similar surface areas in the aqueous solution of NaI (pH = 11, by NaOH). The photocurrent over the anatase TiO_2-A2 electrode was markedly increased by the addition of I^- to the solution, as shown in Figure 8a. Almost 100% of the photogenerated holes over the anatase electrode was consumed for the production of IO_3^- in the presence of 10 mM I^-, as shown in Figure 9. This reaction was carried out under UV irradiation and with an anodic bias (0 V vs Ag/AgCl). These results suggest that the oxidation of I^- mainly proceeded over the TiO_2-A2 photocatalyst in the aqueous solution containing more than 10 mM I^-. This agrees with the result that O_2 evolution was negligible over the TiO_2-A2 photocatalyst in the presence of more than 10 mM I^-, as shown in Figure 4a. Clearly, the I^- anions act as a strong hole scavenger on TiO_2-anatase.

On the other hand, the increase of a photocurrent over the TiO_2-R1 electrode was negligibly small in the presence of 10 mM I^-, as shown in Figure 8b. Approximately 80% of the photogenerated holes was consumed to produce O_2, while the remainder were consumed to produce IO_3^-. Although both the photocurrent and the percentage of I^- oxidation gradually increased with the rising I^- concentration, the oxidation of water proceeded over the rutile electrode even in the presence of 50

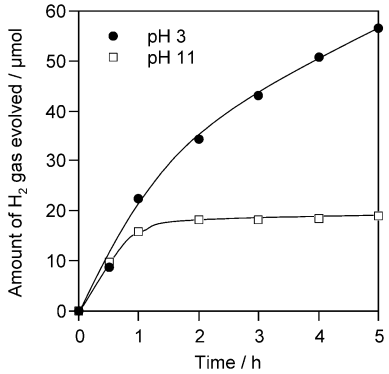

Figure 10. Time course of photocatalytic evolution of H_2 using a Pt-(0.5 wt %)-TiO_2-A1 (Anatase, Ishihara ST-01) photocatalyst suspended in 0.1 M NaI aqueous solution under UV light irradiation (λ > 300 nm, 400 W Hg lamp).

mM I^-. This also agreed with the results on the O_2 evolution over TiO_2-R1, as shown in Figure 4b.

These results clearly indicate that anatase and rutile have a different reactivity in the oxidation of I^- and water. Extensive studies had been made on the competitive oxidation of I^- and water over TiO_2-rutile photoanode,[24−26] but there are no reports regarding a TiO_2-anatase photoanode that we know of. Ohno and co-workers have also reported the preferential oxidation of water over TiO_2-rutile powder photocatalysts in the presence of an Fe^{3+}/Fe^{2+} redox couple.[27] Therefore, rutile itself surely possesses an active site for the effective oxidation of water, as suggested by some researchers. For example, Nakato and co-workers have suggested that the (100) face of TiO_2-rutile possesses favorable properties for water oxidation.[28] Ohno and co-workers have studied the roles of the crystal faces of anatase and rutile particles in photocatalytic reactions. They suggest that the crystal faces help in the separation of electrons and holes. This effect is stronger for the rutile particles than for the anatase particles.[29] Further studies to explain the different reactivity of anatase and rutile are now under investigation.

From these results, we can conclude that the reasons for the efficient and selective water oxidation over the TiO_2-rutile photocatalyst using IO_3^- as an electron acceptor are (i) preferential adsorption properties of IO_3^- anions that enable efficient consumption of photoexcited electrons generated over TiO_2-rutile and (2) the oxidation property of TiO_2-rutile itself that enables the thermodynamically less favorable water oxidation in the presence of an I^- electron donor.

Photocatalytic H_2 Evolution over Pt-Loaded TiO_2-Anatase Photocatalyst using I^- as an Electron Donor under UV Light Irradiation. The results in Figures 4 and 9 indicate that I^- anions act as an effective electron donor over TiO_2-anatase. Thus, we examined a photocatalytic reduction of water to H_2 over TiO_2-anatase photocatalysts using the I^- anion as an electron donor and found that the Pt-loaded TiO_2-anatase photocatalysts showed activity for H_2 evolution under UV light irradiation. Figure 10 presents the time courses of the H_2 evolution over Pt(0.5 wt %)-TiO_2-A1 suspended in a NaI (0.1 M) aqueous solution with different pH values. In an acidic aqueous solution of pH < 5, the I_3^- anion was mainly produced as the oxidation product with H_2 evolution, as reported by Ohno and co-workers.[30] We found that the IO_3^- anion was produced over TiO_2-anatase photocatalyst as the oxidation product of I^- in a basic solution of pH > 9. In solutions of pH 5 to ~9, both I_3^- and IO_3^- were produced. These results indicate that the following reactions had taken place over a TiO_2-anatase photocatalyst under UV light irradiation

$$2H^+ + 2e^- \rightarrow H_2 \text{ (reduction of water to } H_2 \text{ by electrons)} \quad (6)$$

$$3I^- + 2h^+ \rightarrow I_3^- \text{ (oxidation of } I^- \text{ to } I_3^- \text{ by holes)} \quad (7)$$

$$I^- + 6OH^- + 6h^+ \rightarrow IO_3^- + 3H_2O \text{ (oxidation of } I^- \text{ to } IO_3^- \text{ by holes)} \quad (8)$$

The IO_3^- anions in basic solution were possibly produced via the following disproportional reaction from I_3^-:

$$3I_3^- + 6OH^- \rightarrow 8I^- + IO_3^- + 3H_2O \quad (9)$$

The rates of H_2 evolution gradually decreased with the irradiation time, as shown in Figure 10. The H_2 evolution terminated when the concentration of the products (I_3^- or IO_3^-) in the solution reached a certain level. These results indicate that the backward reactions, the reduction of I_3^- (reaction 5) or IO_3^- (reaction 2), proceeded over the reduction site of the photocatalyst. The facile termination of H_2 evolution in the basic solution clearly proves that the IO_3^- anions react more efficiently than I_3^-, as discussed in a previous section.

Simultaneous Evolution of H_2 and O_2 using a Mixture of Pt-TiO_2-Anatase and TiO_2-Rutile under UV Light Irradiation. We attempted water splitting using a combination of Pt-TiO_2-anatase for H_2 evolution and TiO_2-rutile for O_2 evolution, respectively. As shown in Table 2, the combinations of Pt-TiO_2-anatase and bare TiO_2-rutile photocatalysts exhibited simultaneous evolution of H_2 and O_2 with a stoichiometric ratio from basic NaI aqueous solutions (0.1 M, pH = 11). No simultaneous evolutions of H_2 and O_2 were observed when each photocatalyst was used separately or in combination, such as Pt-TiO_2-anatase and bare TiO_2-anatase. Figure 11 shows the time course of gas evolution using the mixture of Pt(0.5 wt %)-TiO_2-A1 and TiO_2-R2, suspended in a basic aqueous solution of NaI (0.1 M, pH = 11), in which simultaneous evolution of H_2 and O_2 with a stoichiometric ratio was observed. The rate of gas evolution gradually decreased with gas accumulation in the closed system because the backward reaction from H_2 and O_2 into H_2O took place on Pt metal particles.[1,31,32] However, the initial rate of gas evolution was recovered by the evacuation of evolved gases. When a 200 h long-term photoreaction was carried out in an aqueous solution of NaI (40 mM, pH = 11) with periodical evacuation of the gas phase, the total amount of H_2 and O_2 reached ca. 15.6 and 7.8 mmol, respectively. The amount of H_2 gas evolved exceeded the stoichiometric amount of TiO_2 powder (6.3 mmol) and I^- (14 mmol) in the solution. No structural change of the TiO_2 photocatalysts was observed after the reaction. These results clearly indicate that both H_2 and O_2 evolutions proceeded photocatalytically. The stoichiometric evolution of H_2 and O_2 was also observed in the case of aqueous LiI and KI solutions but not in the case of NaBr, NaCl, or NaOH solutions. From these results, we can conclude that the overall water splitting proceeds by the redox cycle between IO_3^- reduction and I^- as follows: (i) water reduction to H_2 and I^- oxidation to IO_3^- over Pt-TiO_2-anatase and (ii) IO_3^- reduction to I^- and water oxidation to O_2 over TiO_2-rutile. It should be noted that the rate of H_2 evolution over the combination of Pt-TiO_2-anatase and bare TiO_2-rutile was higher than over Pt-TiO_2-antase alone, as shown in Table 2. The prompt reduction of IO_3^- to I^- over TiO_2-rutile, indicated by the result in Figure 6b, kept the concentration of IO_3^- in the solution very low during photoreaction. Consequently, the IO_3^- reduction to I^- over Pt-TiO_2-anatase, the undesirable backward reaction to

TABLE 2: Photocatalytic Activities of Various Photocatalysts Suspended in NaI Aqueous Solution under UV Light Irradiation*a*

photocatalyst	rates of gas evolution[b] (μmol h^{-1}) H_2	O_2
Pt(0.5 wt %)-TiO_2-A1	20[c]	tr.[d]
Pt(0.5 wt %)-TiO_2-A2	6e	tr.
TiO_2-A1	0	0
TiO_2-A2	0	0
Pt(0.5 wt %)-TiO_2-R1	tr.	0
Pt(0.5 wt %)-TiO_2-R2	tr.	0
TiO_2-R1	0	0
TiO_2-R2	0	0
Pt(0.5 wt %)-TiO_2-A1 + TiO_2-R1	125	62
Pt(0.5 wt %)-TiO_2-A1 + TiO_2-R2	220	110
Pt(0.5 wt %)-TiO_2-A2 + TiO_2-R1	8	4
Pt(0.5 wt %)-TiO_2-A2 + TiO_2-R2	18	9
Pt(0.5 wt %)-TiO_2-R1 + TiO_2-A1	tr.	tr.
Pt(0.5 wt %)-TiO_2-A2 + TiO_2-A2	tr.	tr.
Pt(0.5 wt %)-TiO_2-A1 + Pt(0.5 wt %)-WO_3	95	47[e]
Pt(0.5 wt %)-TiO_2-A1 + Pt(0.5 wt %)-$BiVO_4$	tr.	0

[a] Catalyst: 0.5 g (in the case of mixture 0.25 + 0.25 g); water: 400 mL; NaI: 40 mmol; Pyrex reactor of inner irradiation type; high-pressure Hg lamp (400 W). [b] Rate in steady state. [c] Initial rate. [d] pH 11 adjusted by NaOH. [e] Without pH adjustment.

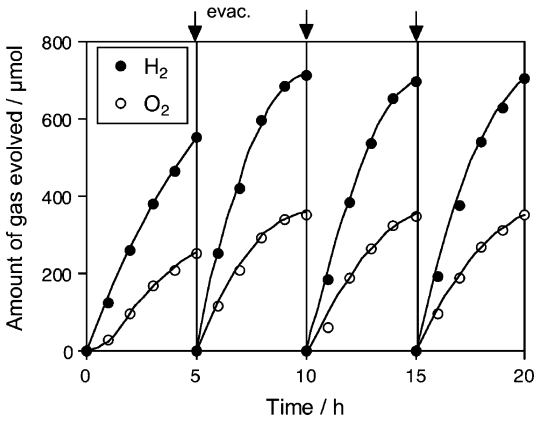

Figure 11. Time course of photocatalytic evolution of H_2 and O_2 using a mixture of Pt-TiO_2-A1 and TiO_2-R2 photocatalysts suspended in 0.1 M NaI aqueous solution (pH 11, adjusted by NaOH) under UV irradiation.

decrease the rate of H_2 evolution, was minimized when the combination of Pt-TiO_2-anatase and bare TiO_2-rutile was used.

The quantum efficiency of overall water splitting was ca. 4% at 350 nm using the combination of Pt(0.5 wt %)-TiO_2-A1 and TiO_2-R2 suspended in a basic aqueous solution of NaI (0.1 M, pH = 11). When Pt(0.5 wt %)-TiO_2-A1 was independently used in a basic aqueous solution of NaI (0.1 M, pH = 11), the quantum efficiency for the initial rate of H_2 evolution was determined to be ca. 1% at 350 nm. On the other hand, ca. 10% of high quantum efficiency was observed in O_2 evolution over TiO_2-R2 in a 2.5 mM $NaIO_3$ aqueous solution (pH = 11) and was ca. 4% in the aqueous mixture of 2.5 mM $NaIO_3$ and 0.1 M NaI (pH = 11). From these results, the H_2 and IO_3^- production over Pt-TiO_2-anatase is the rate-determining step in this water splitting system. Therefore, the total water splitting reaction will proceed more efficiently by improvement of the H_2 evolution system.

The simultaneous evolution of H_2 and O_2 was also observed by using a Pt-WO_3 photocatalyst for O_2 evolution instead of TiO_2-rutile, as shown in Table 2. The reaction was carried out in an aqueous NaI solution with neutral pH condition because WO_3 is unstable in basic conditions. Steady gas evolution was not observed when using Pt-$BiVO_4$. These results clearly indicate that the selective O_2 evolution ability from the aqueous solution containing both IO_3^- and I^- is indispensable for the photocatalyst used as an O_2 evolution system in the present water splitting reaction. The Pt-WO_3 photocatalyst as well as TiO_2-rutile can be used as a photocatalyst for an O_2 evolution system.

Effects of pH and NaI Concentration on Water Splitting using a Combination of Pt-TiO_2-Anatase and TiO_2-Rutile. Figure 12a shows the rates of gas evolution over the mixture of Pt(0.5 wt %)-TiO_2-A1 and bare TiO_2-R2 suspended in 0.1 M NaI aqueous solutions with different pH values. The rates significantly increased with the increase of the pH value from 3 to 9 and decreased again above pH 11. The O_2 evolution was negligible at pH 3 because the main oxidative product over Pt-TiO_2-A1 was I_3^-, which cannot work as an efficient electron acceptor for O_2 evolution over TiO_2-R2, as described previously. At pH 5 to ~7, O_2 evolution was observed after some induction period. The amount of O_2 evolved was less than the stoichiometric ratio to the H_2 evolved because of the accumulation of I_3^- in the solution. The accumulation of I_3^- also causes a light loss due to the strong absorption of the I_3^- anion around 350 nm, resulting in a lower efficiency of the photocatalytic reaction. In basic conditions of pH ≥ 9, the simultaneous evolution of H_2 and O_2, with a stoichiometric ratio (2:1), was observed during the initial period. The gas evolution rates were much higher than those in acidic conditions. These results indicate that a basic condition is more favorable for efficient water splitting because the redox cycle of IO_3^-/I^- has mainly taken place.

The rate of water splitting over the mixture of Pt(0.5 wt %)-TiO_2-A1 and bare TiO_2-R2 was examined in aqueous solutions (pH = 11, by NaOH) with different concentrations of NaI (0 to ~100 mM). No O_2 evolved in the absence of I^- and only small amounts of H_2 evolved. As shown in Figure 12b, the rate of water splitting greatly increased with the increase in NaI concentration, up to 40 mM, and gradually decreased above 40 mM. The presence of I^- anions, even at such low concentrations as 10 mM, results in the water splitting in a stoichiometric ratio ($H_2/O_2 = 2$). As for the H_2 evolution over Pt(0.5 wt %)-TiO_2-A1 alone, the rate of H_2 evolution increased with the increase in the NaI concentration up to 40 mM. As suggested previously, the H_2 evolution over Pt-TiO_2-anatase is the rate-determining step in overall water splitting. Therefore, the rate of overall water splitting appreciably increased with the increase of the H_2 evolution rate over Pt-TiO_2-A1. However, the higher concentration of I^- results in the decrease of the O_2 evolution rate over TiO_2-R2 because of the competitive oxidation of I^- with the oxidation of water, as indicated by the results in Figures 4b and 9. Thus, the efficiency of overall water splitting gradually dropped with the increase in the NaI concentration above 40 mM. In the two-step water splitting system using a redox couple, the concentration of the redox is a significant factor determining the efficiency of the overall reaction.

Simultaneous Evolution of H_2 and O_2 under Visible Light Irradiation using a Combination of Two Visible-Light Driven Photocatalysts. Finally, we investigated visible light-driven photocatalysts with H_2 production ability in the presence of an I^- electron donor to achieve water splitting under visible light with the O_2 evolution photocatalyst Pt-WO_3. We found that Pt-loaded $SrTiO_3$ codoped with Cr and Ta (denoted as $SrTiO_3$:Cr/Ta) showed an activity for both H_2 and IO_3^- production from aqueous NaI solution under visible light irradiation (λ > 420 nm), as shown in Figure 13. This photocatalyst was originally developed by Kudo and co-workers

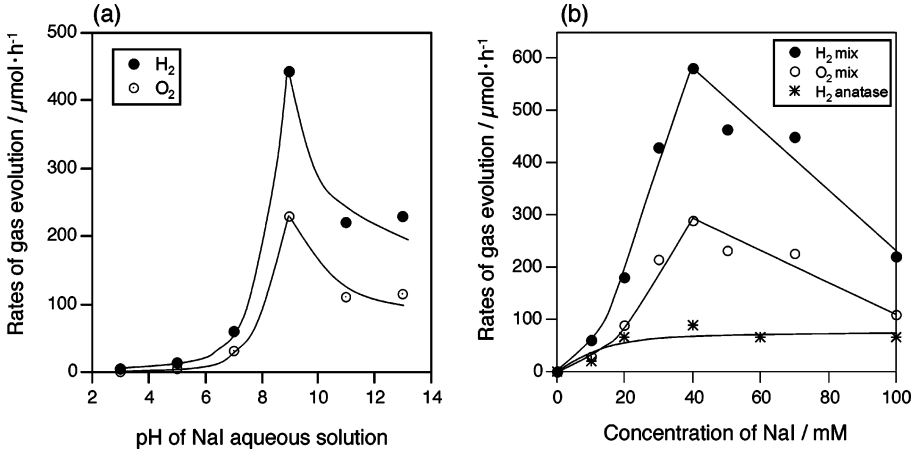

Figure 12. (a) Dependence of rates of gas evolution over a mixture of Pt-TiO_2-A1 and TiO_2-R2 photocatalysts upon the pH value of NaI solution (NaI: 0.1 M). (b) Dependence of rates of gas evolution over a mixture of Pt-TiO_2-A1 and TiO_2-R2 photocatalysts upon the concentration of NaI aqueous solution (pH 11).

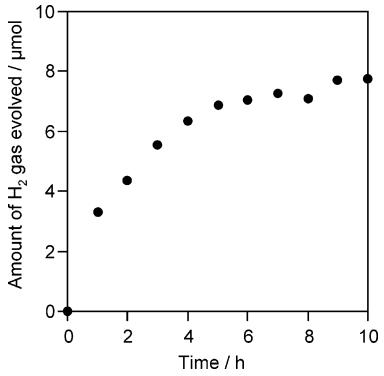

Figure 13. Time course of photocatalytic evolution of H_2 using Pt-(0.3 wt %)-$SrTiO_3$ (Cr, Ta 4 mol % doped) photocatalyst suspended in 30 mM NaI aqueous solution (pH 6.5 without adjustment) under visible light irradiation (λ > 420 nm).

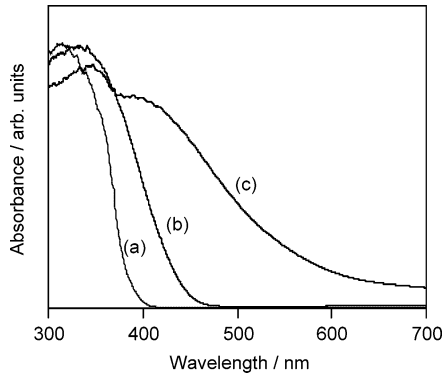

Figure 14. Diffuse reflection spectra of (a) $SrTiO_3$, (b) WO_3, and (c) $SrTiO_3$ codoped with Cr(4%)/Ta(4%).

for the photocatalytic H_2 production from water under visible light irradiation using methanol as a sacrificial electron donor.[22,23] The UV−vis spectra of WO_3, $SrTiO_3$, and $SrTiO_3$:Cr/Ta are presented in Figure 14. $SrTiO_3$:Cr/Ta showed broad adsorption in the visible region up to ca. 600 nm and actually exhibited photocatalytic activity under visible light even through a 500 nm cutoff filter. As shown in Figure 15, the combinations of the Pt(0.3 wt %)- $SrTiO_3$:Cr/Ta and Pt(0.5 wt %)-WO_3 photocatalysts exhibited simultaneous H_2 and O_2 evolution (initial rate H_2: 16 μmol/h and O_2: 8 μmol/h) from NaI aqueous solutions (5 mM, pH = 7) under the visible light irradiation (λ > 420 nm). No gas evolution was observed in darkness (fifth

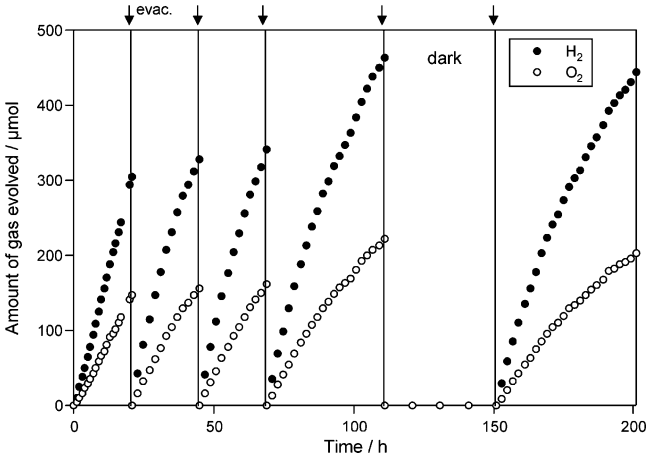

Figure 15. Time course of photocatalytic evolution of H_2 and O_2 using a mixture of Pt(0.3 wt %)-$SrTiO_3$ (Cr, Ta 4 mol % doped) and Pt(0.5 wt %)-WO_3 photocatalysts suspended in 5 mM NaI aqueous solution (pH 6.5 without adjustment) under visible light irradiation (λ > 420 nm).

run). The reaction proceeded without notable deactivation even in long-term reactions, as shown in Figure 15. The total amount of H_2 gas evolved reached ca. 1.9 mmol, exceeding the stoichiometric amount of the photocatalysts ($SrTiO_3$:Cr/Ta: 1.1 mmol and WO_3: 1.4 mmol) and I^- (1.25 mmol) in the solution. The reaction mechanism is certainly the same as that of the Pt-TiO_2-anatase/TiO_2-rutile system. That is, the H_2 and IO_3^- production proceeded over the Pt-$SrTiO_3$:Cr/Ta photocatalyst. The IO_3^- reduction and water oxidation to O_2 take place over Pt-WO_3 under visible light irradiation. The quantum efficiency for overall water splitting was determined to be ca. 1% at 420 nm with the same conditions as in Figure 15.

Figure 16 shows the dependence of gas evolution rates over the combination of Pt-$SrTiO_3$:Cr/Ta and Pt-WO_3 photocatalysts upon the dopants on $SrTiO_3$:Cr/Ta. The equal molar amounts of Ta to Cr were codoped to $SrTiO_3$. The rates of gas evolution increased with the increasing amount of Cr doped up to 4 mol %. Further amounts of doping decreased the efficiency. Kudo and co-workers reported a similar trend for H_2 evolution over a $SrTiO_3$:Cr/Ta photocatalyst using methanol as a sacrificial electron donor.[23] The increase in the doping amount of Cr enhances visible light absorption. However, it works as a recombination center between photogenerated electrons and holes. Consequently, volcano-type dependence was obtained.

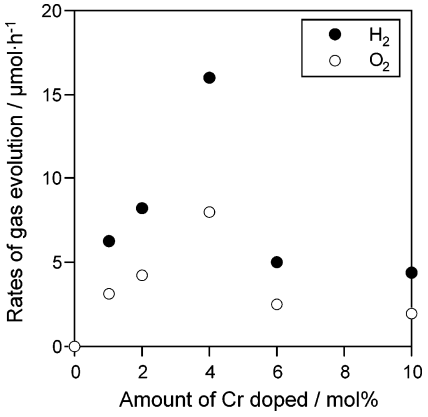

Figure 16. Dependence of rates of gas evolution over a mixture of Pt-$SrTiO_3$ (Cr, Ta doped) and Pt-WO_3 photocatalysts upon the amount of chromium.

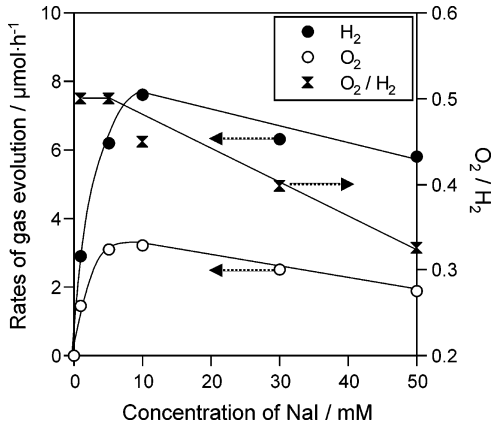

Figure 17. Dependence of rates of gas evolution over a mixture of Pt-$SrTiO_3$ (Cr, Ta 1 mol % doped) and Pt-WO_3 photocatalysts upon the concentration of NaI aqueous solution (without pH adjustment).

Effects of NaI Concentration on Water Splitting using a Combination of Pt-$SrTiO_3$:Cr/Ta and Pt-WO_3 under Visible Light Irradiation. The rate of water splitting over the mixture of Pt(0.5 wt %)-$SrTiO_3$:Cr(1%)/Ta(1%) and Pt(0.5 wt %)-WO_3 was examined in aqueous solutions (pH ~7, without adjustment) with different concentrations of NaI (0 to ~50 mM) under visible light irradiation (λ > 420 nm). Gas evolutions were not observed in the absence of I^-. The rates of gas evolution increased with increasing I^- concentration up to 10 mM and gradually decreased with further concentration, as shown in Figure 17. The decrease is due to the competitive oxidation of I^- over the Pt-WO_3 photocatalysts, which decrease the rate of O_2 evolution, as indicated by the result in Figure 5. The decrease of gas evolution rates with high I^- concentration was also observed in the combination of Pt-TiO_2-anatase and TiO_2-rutile, shown in Figure 12b. However, in the present system, the ratio of H_2 and O_2 gases evolved was not stoichiometric (O_2/H_2 = 0.5) with the I^- concentration above 10 mM, as shown in Figure 17. The O_2/H_2 value decreased with the increasing I^- concentration above 10 mM, and accumulations of I_3^- were confirmed after the reactions. It should be noted that the reaction was carried out in a neutral condition around pH 7 because WO_3 is unstable in basic solutions. In a neutral condition, the oxidation products of I^- over Pt-WO_3 are both I_3^- and IO_3^-. The produced I_3^- anions accumulate in the solution because I_3^- cannot work as an efficient electron acceptor. As mentioned previously, a basic pH condition is favorable for the Pt-TiO_2-anatase/TiO_2-rutile system. The rates of gas evolution were drastically improved with the change of pH from 7 to 9. Therefore, the development of a visible-light driven photocatalyst with both good stability in basic solution and good selectively for water oxidation is strongly desired to improve the efficiency of overall water splitting under visible light irradiation.

Conclusion

A novel photocatalytic system that splits water into H_2 and O_2 was realized using a two-step photoexcitation system composed of an IO_3^-/I^- redox mediator and two different semiconductor photocatalysts. This reaction mechanism is new and significantly different from the conventional water splitting system. We demonstrated photocatalytic water splitting into H_2 and O_2 under visible light irradiation (λ > 420 nm) for the first time by using the IO_3^-/I^- redox couple, Pt-$SrTiO_3$:Cr/Ta for H_2 evolution and Pt-WO_3 for O_2 evolution. Our main conclusions are summarized as follows.

(i) Selective O_2 evolutions proceeded over TiO_2-rutile and Pt-WO_3 photocatalysts using the IO_3^- anion as an electron acceptor under UV light and visible light irradiation, respectively. The characteristic property of this reaction is that the water oxidation to O_2, a thermodynamically less favorable reaction as compared to the oxidation of I^-, proceeds efficiently even in the presence of a considerable amount of I^- anions. The selective O_2 evolution is the key property for the construction of our two-step water splitting system. (ii) The IO_3^- anions easily adsorbed onto the surface of the photocatalysts and efficiently reacted with photoexcited electrons there. The TiO_2-rutile photocatalysts possess unique reactivity in oxidation, enabling preferential water oxidation in the presence of I^-. (iii) Pt-TiO_2-anatase and Pt-$SrTiO_3$:Cr/Ta photocatalysts exhibited good activity for H_2 production from water in the presence of an I^- electron donor under UV light and visible light irradiation, respectively. The oxidation products of I^- were mainly I_3^- in acidic solutions and IO_3^- in basic solutions. (iv) Efficient evolutions of H_2 and O_2 were observed over the mixture of Pt-TiO_2-anatase and bare TiO_2-rutile suspended in NaI aqueous solutions under UV light irradiation. The combination of Pt-$SrTiO_3$:Cr/Ta and Pt-WO_3 photocatalysts demonstrated the photocatalytic water spitting into H_2 and O_2 under visible light irradiation. (v) The efficiency of the overall water splitting reaction was significantly affected by the pH value of the NaI aqueous solution. The basic condition is more favorable for efficient water splitting because the redox cycle of IO_3^-/I^- has mainly taken place. On the contrary, the efficiency in acidic condition was lower than that in the basic condition because of the accumulation of I_3^- anion that could not work as an efficient electron acceptor.

Acknowledgment. This work was supported by the Fund for Young Researchers, Ministry of Education, Culture, Sports, Science, and Technology.

References and Notes

(1) Sato, S.; White, J. M. *Chem. Phys. Lett.* **1980**, *72*, 83−86.

(2) Lehn, J.-M.; Sauvage, J.-P.; Ziessel, R. *Nouv. J. Chim.* **1980**, *4*, 623−627.

(3) Domen, K.; Kudo, A.; Onishi, T.; Kosugi, N.; Kuroda, H. *J. Phys. Chem.* **1986**, *90*, 292−295.

(4) Kudo, A.; Sayama, K.; Tanaka, A.; Asakura, K.; Domen, K.; Muruya, K.; Onishi, T. *J. Catal.* **1989**, *120*, 337−352.

(5) Inoue, Y.; Ogura, S.; Kohno, M.; Sato, K. *Appl. Surf. Sci.* **1997**, *121/122*, 521−524.

(6) Inoue, Y.; Kohno, M.; Kaneko, T.; Ogura, S.; Sato, K. *J. Chem. Soc., Faraday Trans.* **1998**, *94*, 89−94.

(7) Takata, T.; Shinohara, K.; Tanaka, A.; Hara, M., Kondo, J. N.; Domen, K. *J. Photochem. Photobiol., A* **1997**, *106*, 45−49.

(8) Kim, H. G.; Hwang, D. W.; Kim, J.; Kim. Y. G.; Lee, J. S. *Chem. Commun*. **1999**, 1077−1078.
(9) Kudo, A.; Kato, H.; Nakagawa, S. *J. Phys. Chem. B* **2000**, *104*, 571−575.
(10) Kato, H.; Asakura, K.; Kudo, A. *J. Am. Chem. Soc*. **2003**, *125*, 3082−3089.
(11) Bard, A. J. *J. Photochem.* **1979**, *10*, 59−75.
(12) Tennakone, K.; Pushpa, S. J. *Chem. Soc., Chem. Commun*. **1985**, 1435−1437.
(13) Tennakone, K.; Wickramanayake, S. *J. Chem. Soc., Faraday Trans. 2*, **1986**, *82*, 1475−1479.
(14) Tennakone, K.; Tantrigoda, R.; Abeysinghe, S.; Punchiheya, S., Fernando, C. A. N. *J. Photochem. Photobiol., A* **1990**, *52*, 43−46.
(15) Sayama, K.; Yoshida, R.; Kusama, H.; Okabe, K.; Abe, Y.; Arakawa, H. *Chem. Phys. Lett.* **1997**, *277*, 387−390.
(16) Fujihara, K.; Ohno, T.; Matsumura, M. *J. Chem. Soc., Faraday Trans*. **1998**, *94*, 3705−3709.
(17) Ohno, T.; Fujihara, K.; Sarukawa, K.; Tanigawa, F.; Matsumura, M. *Z. Phys. Chem.* **1999**, *213*, 165−174.
(18) Abe, R.; Sayama, K.; Domen, K.; Arakawa, H. *Chem. Phys. Lett*. **2001**, *344*, 339−344.
(19) Sayama, K.; Mukasa, K.; Abe, R.; Abe, Y.; Arakawa, H. *Chem. Commun*. **2001**, 2416−2417.
(20) Kudo, A.; Kato, H.; Tsuji, I. *Chem. Lett.* **2004**, *33*, 1534−1535.
(21) Kudo, A.; Omori, K.; Kato, H. *J. Am. Chem. Soc*. **1999**, *121*, 11459−11467.
(22) Ishii, T.; Nakagawa, S.; Kato, H.; Kudo, A. *Abstract of the Japan Chemical Society Spring Meeting*; 2000; Vol. 78, p 32.
(23) Ishii, T.; Kato, H.; Kudo, A. *J. Photochem. Photobiol., A* **2004**, *163*, 181−186.
(24) Fujishima, A.; Inoue, T.; Honda, K. *J. Am. Chem. Soc*. **1979**, *101*, 5582−5588.
(25) Kobayashi, T.; Yoneyama, H.; Tamura, H. *J. Electroanal. Chem*. **1981**, *122*, 133−145.
(26) Gutierrez, C.; Salvador, P. *J. Electrochem. Soc*. **1986**, *133*, 924−929.
(27) Ohno, T.; Haga, D.; Fujihara, K.; Kaizaki, K.; Matsumura, M. *J. Phys. Chem. B* **1997**, *101*, 6415−6419.
(28) Tsujiko, A.; Kisumi, T.; Magari, Y.; Murakoshi, K.; Nakato, Y. *J. Phys. Chem. B* **2000**, *104*, 4873−4879.
(29) Ohno, T.; Sarukawa, K.; Matsumura, M. *New J. Chem*. **2002**, *26*, 1167−1170.
(30) Ohno, T.; Saito, S.; Fujihara, K.; Matsumura, M. *Bull. Chem. Soc. Jpn.* **1996**, *69*, 3059−3064.
(31) Moon, S. C.; Mametsuka, H.; Tabata, S.; Suzuki, E. *Catal. Today* **2000**, *58*, 125−132.
(32) Abe, R.; Sayama, K.; Arakawa, H. *Chem. Phys. Lett.* **2003**, *371*, 360−364.